International Journal of Research in Engineering and Science (IJRES)
ISSN (Online): 2320-9364, ISSN (Print): 2320-9356
www.ijres.org Volume 14 Issue 7 ǁ July 2026 ǁ PP. 112-126

A Simplified Analytical Method for Assessing Pressure Vessel Nozzles Subjected to Imposed Piping Loads

*Walther Stikvoort
Independent Subject Matter Expert - Pressure Equipment Design & Integrity

Farzad Gardaneh
Senior Static Equipment Engineer, Tehran, Iran
** Corresponding Author: Walther Stikvoort, Wagnerlaan 37, 9402 SH Assen, The Netherlands*

Abstract: *The evaluation of external piping loads acting on pressure vessel nozzles remains an important aspect of mechanical design, directly influencing the structural integrity of nozzle-to-shell intersections. While detailed analytical procedures such as those presented in WRC Bulletins 107, 297, and 368 are widely accepted, they often require iterative calculations or specialized software, making them less suitable for rapid design verification. This paper presents a simplified analytical method for assessing piping loads imposed on flush radial nozzles attached to cylindrical and spherical pressure vessels, with or without reinforcing pads. The method is applicable provided that the shear stresses resulting from transverse forces and torsional moments at the nozzle–shell interface do not exceed 15% of the allowable design stress.*

The proposed methodology combines classical pressure-area reinforcement concepts with simplified stress formulations for pressure, external forces, and bending moments. Effective shell and nozzle lengths are introduced through efficiency factors that account for geometric characteristics and applicable design code requirements. A unified set of equations is developed for determining the pressure stress at the nozzle intersection, calculating the maximum allowable working pressure (MAWP), and evaluating combined stresses against permissible design limits. The method further incorporates the beneficial contribution of reinforcing pads by increasing the effective load-carrying area while requiring an additional assessment of the shell-to-pad transition.

By emphasizing the relationship between reinforcement area and pressure-loaded area, the method provides clear physical insight into nozzle strength while maintaining a conservative design philosophy. The resulting procedure offers a practical alternative to existing WRC methods for routine engineering applications, enabling designers to perform consistent and rapid evaluations of nozzle loading without sacrificing structural reliability or safety.

Keywords: *Pressure vessels; External piping loads; Nozzle-to-shell intersection; Reinforcing pads; Stress analysis; Maximum Allowable Working Pressure (MAWP); Simplified analytical method; WRC Bulletins.*

Date of Submission: 13-07-2026 Date of Acceptance: 24-07-2026

I. DISCUSSION

The analytical method presented in this paper was developed to provide a practical and conservative alternative for evaluating piping loads imposed on pressure vessel nozzles. Its principal objective is not to replace detailed stress analyses where these are warranted, but rather to furnish designers with a transparent and computationally efficient procedure for determining the structural acceptability of nozzle loadings during both preliminary and detailed design. By combining classical pressure vessel reinforcement concepts with simplified analytical stress relationships, the proposed methodology bridges the gap between empirical design rules and the more elaborate procedures represented by WRC Bulletins 107, 297, and 368 [1,2,3].

A distinguishing feature of the method is its direct integration of the pressure-area reinforcement concept [4] into the nozzle load assessment. Pressure vessel design codes have long recognized that the adequacy of a nozzle opening depends on maintaining sufficient reinforcement around the opening to compensate for the removed shell material. The present work extends this concept beyond pressure design by relating the reinforcement geometry to the localized stresses generated by external piping loads. This provides a unified analytical framework in which both pressure loading and externally applied forces and moments are evaluated using the same geometric parameters.

The relationship between the projected pressure-loaded area, (A_p), and the effective load-carrying reinforcement area, (A_f), represents one of the most significant aspects of the methodology. Inspection of the expression

$$\mathrm{MAWP}_{\mathrm{intersection}} = \frac{\mathrm{f_s}}{\left(\frac{\mathrm{A_p}}{\mathrm{A_f}} + 0.5 \right)}$$

shows that the pressure capacity of the nozzle-shell intersection is governed directly by the ratio (A_p /A_f). As this ratio decreases through increased reinforcement or more efficient geometry, the calculated maximum allowable working pressure increases. This behaviour is consistent with established pressure vessel design principles and provides a clear physical interpretation of reinforcement effectiveness. Rather than treating reinforcement as an empirical correction, the proposed formulation explicitly quantifies its contribution to the structural capacity of the nozzle intersection.

The introduction of effective shell and nozzle lengths further contributes to the simplicity and versatility of the method. Instead of assuming that the entire surrounding shell participates in resisting localized loads, the formulation recognises that only a finite region adjacent to the opening contributes significantly to load transfer. The effective lengths are represented by simple expressions based upon shell and nozzle geometry together with efficiency factors that reflect design code requirements. Consequently, the resulting equations remain straightforward while preserving the essential structural behaviour observed in more sophisticated analytical models.

The efficiency factors (k_s), (k_n), and (k_p) provide an effective means of accommodating differences between pressure vessel design codes without altering the underlying methodology. The variation of the shell efficiency factor (k_s) with the dimensionless geometric parameter (δ) reflects the gradual reduction in effective shell participation as nozzle size increases relative to shell dimensions. For relatively small openings the shell behaves efficiently, resulting in (k_s = 1.0). As the opening becomes proportionally larger, the effective reinforcement length decreases until the lower bound of 0.75 is reached. This behaviour is physically consistent with the increasing stress concentration associated with larger nozzle openings. The constant value adopted for the nozzle efficiency factor simplifies the calculations while recognising that nozzle reinforcement effectiveness is less sensitive to geometry than the surrounding shell.

Another important aspect of the proposed methodology is the separate treatment of cylindrical and spherical shells. These geometries possess fundamentally different stress distributions under internal pressure and external loading. Cylindrical shells primarily develop circumferential and longitudinal membrane stresses, whereas spherical shells exhibit a more uniform biaxial stress field. These differences are reflected naturally within the proposed equations through distinct pressure stress expressions, projected pressure areas, and auxiliary geometric relationships. Despite these differences, both shell geometries are evaluated using the same general assessment philosophy, thereby providing a consistent analytical framework applicable to the majority of pressure vessel configurations encountered in industrial practice.

The methodology also explicitly recognises the structural contribution of reinforcing pads. When present, the reinforcing pad increases the effective load-carrying cross-sectional area and therefore improves both pressure resistance and resistance to externally applied piping loads. Unlike some simplified procedures that consider only the local reinforcement effect, the present method additionally requires verification of the transition between the reinforcing pad and the vessel shell. This requirement acknowledges that stress concentrations may shift away from the nozzle-shell junction and become critical at the pad termination if the transition is not properly proportioned. Consequently, the method encourages balanced reinforcement rather than merely increasing pad thickness without considering its structural interaction with the shell.

The simplified stress equations for pressure, external forces, and bending moments constitute another practical advantage of the proposed approach. Each loading component is represented by relatively simple expressions involving auxiliary coefficients that depend only upon shell geometry. These coefficients may readily be calculated using standard spreadsheet software, enabling rapid assessment of numerous loading combinations without requiring finite element analysis or extensive interpolation from published charts. This computational simplicity is particularly advantageous during piping layout studies, where multiple nozzle orientations and support configurations may be evaluated before the final design is established.

The assessment criteria are formulated in terms of combined stresses acting in both the vessel shell and the nozzle neck. By evaluating these locations separately, the method recognises that either component may govern the structural acceptability depending upon the relative shell and nozzle thicknesses. The inclusion of the shell-to-nozzle thickness ratio through the coefficient (c_n) provides a rational means of transferring stress effects between the two structural components while preserving equilibrium between the connected elements. This dual assessment improves confidence that both the shell and the nozzle satisfy the applicable allowable stress limits.

The applicability of the proposed method is intentionally restricted to cases where shear stresses resulting from transverse forces and torsional moments remain below 15% of the allowable design stress. This limitation reflects the assumptions upon which the simplified analytical formulation is based. Within this range, membrane and bending stresses dominate the structural response, allowing the simplified equations to provide conservative and reliable results. Situations involving large torsional moments, substantial local plasticity, highly non-linear behaviour, closely spaced nozzles, or complex shell discontinuities remain more appropriately evaluated using detailed finite element analysis or established WRC[1,2,3] procedures. Consequently, the proposed methodology should be regarded as complementary to, rather than a replacement for, more comprehensive analytical methods.

From an engineering perspective, one of the principal strengths of the proposed procedure is its transparency. Every component of the calculated stress can be traced directly to a corresponding physical parameter, allowing designers to understand how variations in shell thickness, nozzle dimensions, reinforcement geometry, or piping loads influence the final assessment. This transparency facilitates engineering judgement, promotes design optimisation, and simplifies independent verification of calculations. In contrast to methods that rely extensively on interpolation of empirical data or numerical models, the present approach enables engineers to identify immediately the parameters that most strongly influence structural performance.

Although the methodology has been developed using conservative assumptions, additional validation against existing WRC[1,2,3] methods and finite element analyses would further establish its range of applicability. Comparative studies covering a broad spectrum of shell diameters, nozzle sizes, reinforcement configurations, and loading conditions would provide valuable insight into the degree of conservatism inherent in the proposed equations. Such investigations could also identify opportunities for refining individual coefficients while preserving the overall simplicity of the analytical procedure.

Overall, the proposed methodology provides a practical balance between analytical rigour and computational simplicity. It preserves the essential mechanics governing nozzle-shell interactions while eliminating much of the complexity associated with traditional nozzle load evaluation methods. For routine engineering applications where rapid and consistent assessments are required, the procedure offers an efficient alternative that remains firmly grounded in established pressure vessel design principles. Its unified treatment of pressure loading, reinforcement effectiveness, and externally applied piping loads makes it particularly well suited for implementation within modern engineering design workflows, where transparency, repeatability, and ease of application are of equal importance to computational accuracy.

II. METHODOLOGY

The methodology adopted in this study is based on the pressure–area reinforcement approach for evaluating the structural integrity and pressure capacity of flush isolated set-in nozzles attached to cylindrical and spherical pressure vessel shells [4,5]. The analytical procedure quantifies the stresses generated at the nozzle–shell intersection, determines the adequacy of reinforcement, and evaluates the Maximum Allowable Working Pressure (MAWP) in accordance with the equations presented in Tables 1–8.

The analysis considers four nozzle configurations: (1) cylindrical shell without a reinforcing pad, (2) cylindrical shell with a reinforcing pad, (3) spherical shell without a reinforcing pad, and (4) spherical shell with a reinforcing pad. The required geometric parameters, material properties, and design stresses are defined using the nomenclature summarized in Table 4.

II.1 Effective Shell and Nozzle Lengths

The methodology begins by determining the effective shell length (L_s) and effective nozzle length (L_n) using the corresponding efficiency factors k_s and k_n. These efficiency factors are selected according to the governing design code or calculated from the dimensionless geometric parameter δ, as summarized in Table 3. Where a reinforcing pad is present, the reinforcing pad factor k_p and the pad dimensions are incorporated into the calculations.

II.2 Pressure-Loaded Area and Reinforcement Area

Using the calculated effective lengths, the projected pressure-loaded area (A_p) and the available load-carrying cross-sectional area (A_f) are determined from the appropriate expressions for cylindrical or spherical shells. For reinforced nozzles, the contribution of the reinforcing pad is included in the reinforcement area A_f.

The following shall be taken into account: if the design stresses of the nozzle neck and reinforcing pad (where provided) are lower than the shell design stress, the effective load-carrying areas of the nozzle neck and reinforcing pad shall be determined by multiplying their respective areas by the ratio of their design stresses to the shell design stress.

II.3 Maximum Allowable Working Pressure

The pressure capacity of the nozzle intersection is then evaluated by computing the Maximum Allowable Working Pressure at the intersection:

$$\mathrm{MAWP}_{\mathrm{intersection}} = \frac{\mathrm{f_s}}{\left(\frac{\mathrm{A_p}}{\mathrm{A_f}} + 0.5\right)}$$

The MAWP of the undisturbed shell is also calculated using the appropriate expressions for cylindrical and spherical vessels. The governing allowable pressure is taken as the lower value between the nozzle-intersection MAWP and the undisturbed-shell MAWP. Since the intersection MAWP is inversely proportional to the ratio A_p/A_f , increasing the available reinforcement area results in a higher allowable working pressure, thereby improving the structural capacity of the nozzle connection.

II.4 Pressure Stress at the Nozzle Intersection

Pressure stresses produced by the internal design pressure are subsequently calculated using the pressure stress equations presented in Table 1. The auxiliary parameter z, which accounts for shell geometry and reinforcement effectiveness, is first determined and then used to evaluate the membrane pressure stress for either cylindrical or spherical shells.

II.5 Stresses from External Forces and Moments

To assess the structural adequacy of the nozzle under combined loading, additional stresses resulting from external forces and applied moments are calculated using the stress coefficients c_{11}, c_{21}, c_{31}, c_{41}, and c_n (Table 6). For reinforced nozzle connections, the shell thickness is replaced by the combined thickness (t_s+t_p) and the modified auxiliary coefficients listed in Tables 7 and 8 are employed. The transition between the vessel shell and the reinforcing pad is also evaluated to ensure that the reinforcement does not introduce excessive local stresses.

II.6 Assessment Criteria

The combined stresses are then checked against the allowable design stress limits using the assessment criteria summarized in Table 5. Separate stress interaction equations are applied for cylindrical and spherical shells, as well as for the nozzle neck, ensuring that the combined effects of pressure, external loads, and bending moments remain below the allowable stress of the shell or nozzle material.

II.7 Comparative Evaluation of Nozzle Configurations

Finally, the analytical results obtained for the different nozzle configurations are compared to evaluate the influence of shell geometry, reinforcement pads, effective reinforcement lengths, and efficiency factors on the pressure-carrying capacity and stress distribution of nozzle–shell intersections. This systematic procedure provides a consistent basis for assessing the structural performance and safety of pressure vessel nozzle connections under internal pressure and combined mechanical loading.

Table 1. Calculation scheme for determining the pressure stress of a nozzle in a cylindrical or spherical shell

Nozzle in cylindrical shell	Nozzle in spherical shell
Pressure stress cylindrical shell $$\sigma_p = \frac{2.5}{\mathrm{z}} \frac{\mathrm{p_d}}{\mathrm{l_n}\,(\frac{D_o}{D_i})}$$ Auxiliary quantity z $$z = \frac{\mathrm{D_o} - \mathrm{t_s}}{\mathrm{t_s}} \frac{\mathrm{A_f}}{2\mathrm{A_p} + A_f}$$	Pressure stress spherical shell $$\sigma_p = \frac{2.0}{\mathrm{z}} \frac{\mathrm{p_d}}{2.\mathrm{l_n}\,(\frac{D_o}{D_i})}$$ Auxiliary quantity z $$z = 0.5\, \frac{\mathrm{D_o} - \mathrm{t_s}}{\mathrm{t_s}} \frac{\mathrm{A_f}}{2\mathrm{A_p} + A_f}$$

Table 2. Summary of Formulas Supporting the Pressure–Area Methodology

Flush isolated set-in nozzle without reinforcing pad in cylindrical shell	Flush isolated set-in nozzle with reinforcing pad in cylindrical shell
$$\mathrm{L_n} = \mathrm{k_n}\sqrt{(\mathrm{d_n} - \mathrm{t_n})\mathrm{t_n}}$$	

$L_s = k_s \sqrt{(D_o - t_s)t_s}$	
$A_p = \frac{D_i}{2}(L_s + \frac{d_n}{2}) + \frac{d_i}{2}(L_n + t_s)$	
$A_f = t_s \,.\, L_s + (L_n + t_s)\, t_n$	$A_f = t_s \,.\, L_s + (L_n + t_s)\, t_n + k_p\,(L_p \,.\, t_p)$
$MAWP_{\text{intersection}} = \frac{f_s}{(\frac{A_p}{A_f} + 0.5)}$	
$MAWP_{\text{undisturbed shell}} = f_s . l_n\, (\frac{D_o}{D_i})$	

Flush isolated set-in nozzle without reinforcing pad in spherical shell	**Flush isolated set-in nozzle with reinforcing pad in spherical shell**
$L_n = k_n \sqrt{(d_n - t_n)t_n}$	
$L_s = k_s \sqrt{(2R_i + t_s)t_s}$	
$R_m = (R_i + 0.5\, t_s)$	
$\delta = \frac{d_n}{2R_m}$	
$a = R_m \,.\, \arcsin \delta$	
$A_p = 0.5\, R_i^2\, \frac{L_s + a}{0.5t_s + R_i} + 0.5\, d_i\,(L_n + t_s)$	
$A_f t_s \,.\, L_s + (L_n + t_s)\, t_n$	$A_f = t_s \,.\, L_s + (L_n + t_s)\, t_n + k_p\,(L_p \,.\, t_p)$
$MAWP_{\text{intersection}} = \frac{f_s}{\left(\frac{A_p}{A_f} + 0.5\right)}$	
$MAWP_{\text{undisturbed shell}} = 2\, f_s . l_n\, (\frac{D_o}{D_i})$	

From closer examination of the expression for the MAWP at a nozzle-shell intersection in a pressure vessel: $MAWP_{\text{intersection}} = \frac{f_s}{(\frac{A_p}{A_f} + 0.5)}$ it is mathematically evident that as the ratio $\frac{A_p}{A_f}$ decreases, the MAWP increases. This inverse relationship highlights the importance of maximizing the reinforcement area A_f to the projected pressure area A_p to improve the pressure-holding capacity at the nozzle intersection.

Table 3. Overview k-factors

k-factors associated with shell, nozzle neck and reinforcing pad	
k_s (Depending on the design code varying between)	0.75 and 1.0
k_n (Depending on the design code varying between)	0.78 and 1.25
k_p (Depending on the design code varying between)	0.75 and 1.0

The efficiency factors k_s and k_n are determined based on the dimensionless geometric parameter δ, defined as:

$$\delta = \frac{d_i}{\sqrt{(D_o - t_s)\, t_s}}$$

The efficiency factor k_n remains constant for all values of δ and is given by: $k_n = 1.0$
In contrast, the efficiency factor k_s varies as a function of δ, according to the following piecewise definition:

- For $\delta \leq 4$; $k_s = 1.0$
- For $4 < \delta < 16$; $k_s = \frac{13}{12} - \frac{\delta}{48}$
- For $\delta \geq 16$; $k_s = 0.75$

Linear interpolation is permitted for values of δ between 4 and 16 to ensure a smooth transition.
The designer may select k-values freely unless their selection is prescribed by the governing design code or standard.

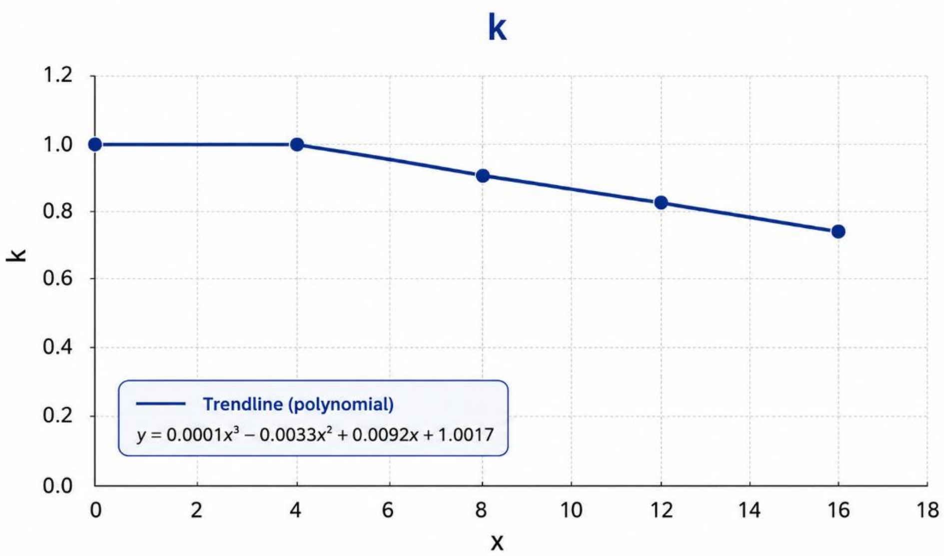

Key: The vertical y-axis represents $k = k_s$, while the horizontal x-axis corresponds to δ

Table 4. Nomenclature

Symbol	Description	Unit
D_o	Outside diameter shell	mm
D_i	Inside diameter shell	mm
R_i	Inside radius sphere	mm
R_m	Mean radius sphere	mm
t_s	Shell thickness	mm
t_n	Nozzle neck thickness	mm
d_n	Outside nozzle diameter	mm
d_i	Inside nozzle diameter	mm
L_p	Width of reinforcing pad	mm
d_p	Outside diameter repad ($2\,L_p + d_n$)	mm
t_p	Thickness of reinforcing pad	mm
L_n	Effective length of nozzle neck	mm
L_s	Effective length of shell	mm
k_s	Shell factor	-
k_n	Nozzle factor	-
k_p	Repad factor	-
A_p	Pressure loaded area	mm^2
A_f	Load - carrying cross- sectional area	mm^2
$MAWP_{intersection}$	Maximum Allowable Working Pressure for nozzle intersection	MPa
$MAWP_{undisturbed\ shell}$	Maximum Allowable Working Pressure for undisturbed shell	MPa
f_s	Design stress shell	MPa
f_n	Design stress nozzle	MPa
f_p	Design stress reinforcing pad	MPa
σ_p	Pressure stress	MPa

l_n	Natural logarithm (-)	-

Figure1. Nozzle configuration on spherical shell

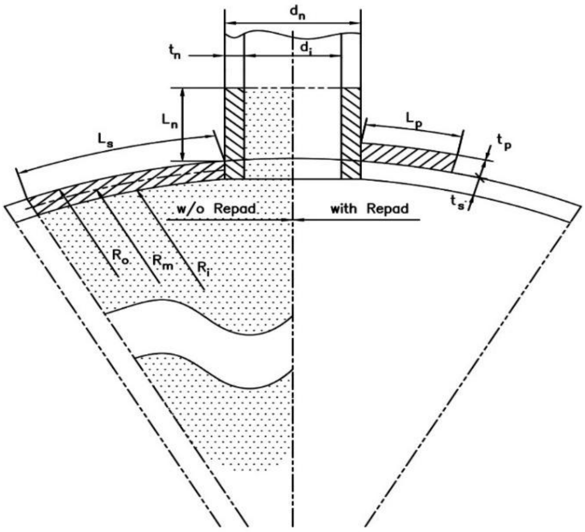

Figure 2. Nozzle configuration on cylindrical shell

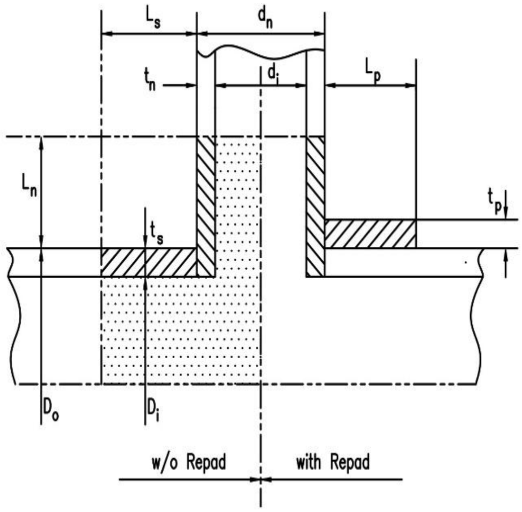

Table 5. Assessment conditions

Cylindrical shell	Spherical shell
$\sigma_p + \sigma_F + \sigma_{Ml} + \sigma_{Mc} \leq 2.85\ f_s$	$\sigma_p + \sigma_F + \sigma_M \leq 2.85 f_s$
Nozzle on cylindrical shell	**Nozzle on spherical shell**
$\sigma_p\sqrt{c_n} + (\sigma_F + \sigma_{Ml} + \sigma_{Mc})c_n \leq 2.85\ f_n$	$\sigma_p\sqrt{c_n} + (\sigma_F + \sigma_M)c_n \leq 2.85\ f_n$
With:	
$\sigma_p = \frac{2.5}{z}\frac{p_d}{l_n\left(\frac{D_o}{D_i}\right)}$	$\sigma_p = \frac{2.0}{z}\frac{p_d}{2.\,l_n\left(\frac{D_o}{D_i}\right)}$
$\sigma_F = 6\ c_{21}\ \lvert F\rvert$	$\sigma_F = 1.75\ c_{21}\ \lvert F\rvert$
$\sigma_{Ml} = 1.5\ c_{31}\ \lvert M_l\rvert$	$\sigma_M = 1.75\ c_{31}\ \lvert M\rvert$
$\sigma_{Mc} = 1.15\ c_{31}\,.\,c_{41}\ \lvert M_c\rvert$	

Table 6. For the auxiliary values c_{11}, c_{21}, c_{31}, c_{41} and c_n in both cases:

$c_{11} = \frac{D_o - t_s}{2t_s}$
$c_{21} = \frac{\sqrt{c_{11}}}{\pi\ t_s d_n}$
$c_{31} = \frac{4\sqrt{c_{11}}}{\pi\ t_s (d_n)^2}$
$c_{41} = \sqrt{\frac{d_n}{2t_s}}$
$c_n = \frac{t_s}{t_n}$

Table 7. In case a reinforcing pad is present then t_s shall be replaced by $(t_s + t_p)$ in the formulas for the auxiliary values c_{11}, c_{21}, c_{31}, c_{41} and c_n
At the same time the transition between vessel shell and the repad shall be assed.

Cylindrical shell	Spherical shell
$\sigma_p + \sigma_F + \sigma_{Ml} + \sigma_{Mc} \leq 2.85\ f_s$	$\sigma_p + \sigma_F + \sigma_M \leq 2.85\ f_s$

With:	With:
$\sigma_p = c_{12} \cdot p_d$	$\sigma_p = \frac{c_{12}}{2} \cdot p_d$
$\sigma_F = 6\, c_{22} \cdot \lvert F \rvert$	$\sigma_F = 1.75\, c_{22} \lvert F \rvert$
$\sigma_{Ml} = 1.5\, c_{32} \lvert M_l \rvert$	$\sigma_M = 1.75\, c_{32} \lvert M \rvert$
$\sigma_{Mc} = 1.15\, c_{42} \cdot c_{32} \lvert M_c \rvert$	

Table 8. For the auxiliary values c_{12}, c_{22}, c_{32} and c_{42} in both cases:

$c_{12} = \frac{D_o - t_s}{2t_s}$
$c_{22} = \frac{\sqrt{c_{12}}}{\pi . t_s . d_p}$
$c_{32} = \frac{4\sqrt{c_{12}}}{\pi . t_s (d_p)^2}$
$c_{42} = \sqrt{\frac{d_p}{2t_s}}$

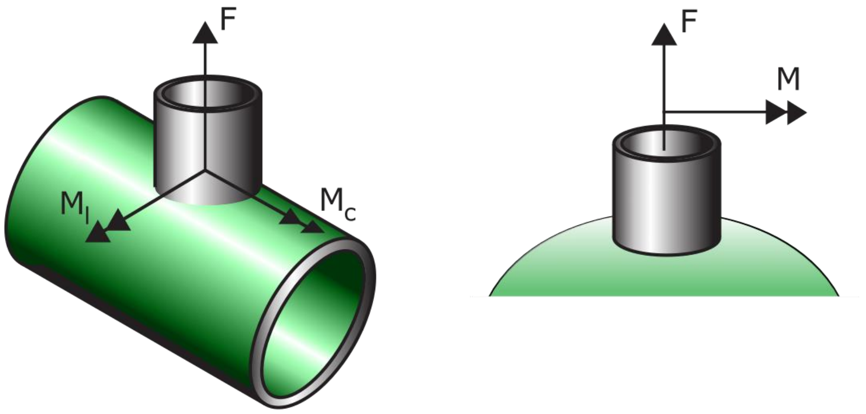

Figure 3. Conventions for applied forces and moments acting on nozzles.

II.8 Worked Example: Pad-Reinforced Set-In Nozzle in a Cylindrical Shell

To illustrate the application of the proposed methodology, the following worked example evaluates a flush set-in nozzle fitted with a reinforcing pad on a cylindrical shell, subjected to internal pressure combined with external piping loads. All input parameters are summarized in Table 9, and the calculation proceeds through Tables 1, 2, 3, 6, 7 and 8 in the sequence described in Sections II.1 to II.6.

Table 9. Input parameters for the worked example

Symbol	Description	Value	Unit
D_o	Shell outside diameter	1220	mm
t_s	Shell thickness	20	mm
D_i	Shell inside diameter (= $D_o - 2t_s$)	1180	mm
d_n	Nozzle outside diameter (DN250 / NB10")	273	mm
t_n	Nozzle neck thickness	12.7	mm
d_i	Nozzle inside diameter (= $d_n - 2t_n$)	247.6	mm
L_p	Reinforcing pad width	100	mm
t_p	Reinforcing pad thickness	16	mm
d_p	Pad outside diameter (= $2L_p + d_n$)	473	mm
p_d	Design pressure	1.5	MPa
f_s	Design stress, shell	138	MPa
f_n	Design stress, nozzle	138	MPa
f_p	Design stress, pad	115	MPa

F	Resultant external force	15000	N
M_l	Longitudinal bending moment	2.0×10^6	N·mm
M_c	Circumferential bending moment	1.5×10^6	N·mm
k_s, k_n, k_p	Efficiency factors (shell, nozzle, pad; geometry/weld-based, Table 3)	1.0 / 1.0 / 1.0	–
f_p/f_s	Pad design-stress ratio (applied to the pad term in A_f, Section II.2)	0.83	–

Step 1 — Efficiency factors and effective lengths:

$$\delta = \frac{d_i}{\sqrt{(D_o - t_s)\, t_s}} = \frac{247.6}{\sqrt{(1220 - 20) \times 20}} = 1.6$$

Since $\delta \le 4$, $k_s = 1.0$ (Table 3); $k_n = 1.0$ (constant), reflecting that the nozzle is of the same material as the shell ($f_n = f_s = 138$ MPa). The reinforcing pad, however, is of a lower-strength material, with design stress $f_p = 115$ MPa. Applying the stress-ratio rule of Section II.2, the pad efficiency factor is therefore $k_p = f_p/f_s = 115/138 = 0.83$, rather than the full-strength value of 1.0.

The effective lengths (Table 2) follow as:

$$L_n = k_n \sqrt{(d_n - t_n)t_n} = 1 \times \sqrt{(273 - 12.7) \times 12.7} = 57.5 \text{ mm}$$
$$L_s = k_s \sqrt{(D_o - t_s)t_s} = 1 \times \sqrt{(1220 - 20) \times 20} = 154.9 \text{ mm}$$

Step 2 — Pressure-loaded area A_p and reinforcement area A_f :

With the pad contribution included, the pressure-loaded and reinforcement areas for a cylindrical shell (Table 2) are:

$$A_p = \frac{D_i}{2}\left(L_s + \frac{d_n}{2}\right) + \frac{d_i}{2}(L_n + t_s) = 590(154.9 + 136.5) + 123.8(57.5 + 20) = 181520 \text{ mm}^2$$

$$A_f = t_s \,.\, L_s + (L_n + t_s)t_n + k_p\left(L_p \,.\, t_p\right) = 20(154.9) + (57.5 + 20)(12.7) + 1.0 \times 0.83(100 \times 16)$$

$$A_f = 5410.25 \text{ mm}^2$$

The area ratio is therefore:

$$\frac{A_p}{A_f} = 33.5$$

Step 3 — Maximum Allowable Working Pressure:

$$\text{MAWP}_{\text{intersection}} = \frac{f_s}{\left(\frac{A_p}{A_f} + 0.5\right)} = \frac{138}{33.5 + 0.5} = 4.06 \text{ MPa}$$

$$\text{MAWP}_{\text{undisturbed shell}} = f_s . l_n \left(\frac{D_o}{D_i}\right) = 138 \times \ln\left(\frac{1220}{1180}\right) = 4.60 \text{ MPa}$$

The nozzle intersection governs, giving an allowable pressure of 4.06 MPa — above the design pressure of p_d = 1.5 MPa, so the pressure design of the connection is acceptable (37% utilization).

Step 4 — Pressure stress at the nozzle intersection:

The auxiliary parameter (Table 1) is:

$$z = \frac{D_o - t_s}{t_s}\frac{A_f}{2A_p + A_f} = \frac{1220 - 20}{20} \times \frac{5410.25}{(2 \times 181520) + 5410.25} = 0.881$$

pressure stress at the intersection is:

$$\sigma_p = \frac{2.5}{z}\frac{p_d}{l_n\left(\frac{D_o}{D_i}\right)} = \frac{2.5}{0.881} \times \frac{1.5}{0.0333} = 127.8 \text{ MPa}$$

Step 5 — Stresses from external forces and moments at the intersection:

Because a pad is present, t_s is replaced by ($t_s + t_p$) = 36 mm in the auxiliary coefficients (Table 7), while the nozzle diameter d_n is retained (Table 6):

$$c_{11} = \frac{D_o - t_s}{2t_s} = \frac{1220 - 36}{2 \times 36} = 16.44$$

$$c_{21} = \frac{\sqrt{c_{11}}}{\pi\, t_s d_n} = \frac{\sqrt{16.44}}{\pi \times 36 \times 273} = 1.31 \times 10^{-4}$$

$$c_{31} = \frac{4\sqrt{c_{11}}}{\pi\, t_s (d_n)^2} = \frac{4\sqrt{16.44}}{\pi \times 36 \times (273)^2} = 1.92 \times 10^{-6}$$

$$c_{41} = \sqrt{\frac{d_n}{2t_s}} = \sqrt{\frac{273}{2 \times 36}} = 1.95$$

$$c_n = \frac{t_s}{t_n} = \frac{36}{12.7} = 2.84$$

The associated stresses (Table 5) are:

$$\sigma_F = 6\, c_{21}\, |F| = 11.8 \text{ MPa}$$
$$\sigma_{Ml} = 1.5\, c_{31}\, |M_l| = 5.8 \text{ MPa}$$
$$\sigma_{Mc} = 1.15\, c_{31} \,.\, c_{41}\, |M_c| = 6.5 \text{ MPa}$$

Step 6 — Combined stress checks:

Shell at the nozzle intersection (Table 5):

$$\sigma_p + \sigma_F + \sigma_{Ml} + \sigma_{Mc} \le 2.85\, f_s$$
$$127.8 + 11.8 + 5.8 + 6.5 = 151.9 \text{ MPa} \le 2.85\, f_s = 393.3 \text{ MPa (39\% utilization)}$$

Nozzle neck:

$$\sigma_p \sqrt{c_n} + (\sigma_F + \sigma_{Ml} + \sigma_{Mc}) c_n \le 2.85\, f_n$$
$$127.8(1.68) + (24.1)(2.84) = 214.8 + 68.2 = 283.0 \text{ MPa} \le 2.85\, f_n = 393.3 \text{ MPa}$$

satisfied, 72% utilization and the governing check in this example.

Pad-to-shell transition (Table 8, using d_p = 473 mm in place of d_n):

$$c_{12} = \frac{D_o - t_s}{2t_s} = 16.44$$

$$c_{22} = \frac{\sqrt{c_{12}}}{\pi\, t_s . d_p} = 7.58 \times 10^{-5}$$

$$c_{32} = \frac{4\sqrt{c_{12}}}{\pi\, t_s (d_p)^2} = 6.41 \times 10^{-7}$$

$$c_{42} = \sqrt{\frac{d_p}{2t_s}} = 2.56$$

giving:

$$\sigma_p = c_{12} \,.\, p_d = 24.7 \text{ MPa}$$
$$\sigma_F = 6\, c_{22} \,.\, |F| = 6.8 \text{ MPa}$$
$$\sigma_{Ml} = 1.5\, c_{32}\, |M_l| = 1.9 \text{ MPa}$$
$$\sigma_{Mc} = 1.15\, c_{42} \,.\, c_{32}\, |M_c| = 2.8 \text{ MPa}$$

So:

$$\sum \sigma_{pad} = 36.2 \text{ MPa} \le 393.3 \text{ MPa (satisfied, 9\% utilization)}$$

Table 10. Summary of results for the worked example

Check	Location	Demand	Limit	Utilization
Pressure capacity	Nozzle intersection (MAWP)	p_d = 1.5 MPa	MAWP = 4.06 MPa	37%
Combined stress	Shell at nozzle intersection	151.9 MPa	$2.85f_s$ = 393.3 MPa	39%
Combined stress	Nozzle neck	283.0 MPa	$2.85f_n$ = 393.3 MPa	72%
Combined stress	Pad-to-shell transition	36.2 MPa	$2.85f_s$ = 393.3 MPa	9%

All four checks are satisfied, with the nozzle neck governing at 72% of its allowable combined stress. The example illustrates how the lower-strength reinforcing pad still meaningfully reduces demand at its own transition to the shell (9% utilization), while the underlying nozzle neck remains the more critical location — precisely the type of insight the proposed pressure-area method is intended to make transparent to the designer.

II.9 Worked Example: Unreinforced Flush Nozzle in a Spherical Shell (Long Weld-Neck Flange)

A second example illustrates the unreinforced (no-pad) spherical-shell branch of the methodology, using a long weld-neck flange as the nozzle. The flange is welded to the shell at the thicker, base section of its tapered hub rather than at the thinner pipe-equivalent end, so the full hub cross-section is credited as local reinforcement. All input parameters are summarized in Table 11.

Table 11. Input parameters for the spherical-shell worked example

Symbol	Description	Value	Unit
R_i	Shell inside radius	734	mm
t_s	Shell thickness	16	mm
D_o	Shell outside diameter (= $2R_i + 2t_s$)	1500	mm
D_i	Shell inside diameter (= $D_o - 2t_s$)	1468	mm
d_n	Nozzle outside diameter (8" NB long weld-neck flange, weld end)	260	mm
t_n	Nozzle wall thickness at shell attachment	20.45	mm
d_i	Nozzle inside diameter (= $d_n - 2t_n$)	219.1	mm
p_d	Design pressure	2.0	MPa
f_s	Design stress, shell	138	MPa
f_n	Design stress, nozzle	138	MPa
F	Resultant external force	10000	N
M	Resultant applied moment	1.5×10^6	N·mm
k_s, k_n	Efficiency factors (shell, nozzle)	1.0 / 1.0	–

Step 1 — Efficiency factors and effective lengths:

$$\delta = \frac{d_i}{\sqrt{(D_o - t_s)t_s}} = \frac{219.1}{\sqrt{1484 \times 16}} = \frac{219.1}{154.1} = 1.42$$

Since:

$$\delta \leq 4$$

the efficiency factors are:

$$k_s = 1.0$$

(from Table 3) and:

$$k_n = 1.0 \text{ (constant)}$$

The effective lengths (Table 2, spherical shell) are therefore:

$$L_n = k_n\sqrt{(d_n - t_n)t_n} = \sqrt{239.55 \times 20.45} = 70 \text{ mm}$$

$$L_s = k_s\sqrt{(2R_i + t_s)t_s} = \sqrt{1484 \times 16} = 154.1 \text{ mm}$$

Step 2 — Pressure-loaded area A_p and reinforcement area A_f:

The spherical-shell geometry additionally requires the mean radius:

$$R_m = R_i + 0.5t_s = 734 + 8 = 742 \text{ mm}$$

The arc length associated with the nozzle opening is:

$$\frac{d_n}{2R_m} = \frac{260}{2 \times 742} = 0.175$$

thus:

$$a = R_m \sin^{-1}\left(\frac{d_n}{2R_m}\right) = 742 \times 0.176 = 130.7 \text{ mm}$$

The pressure-loaded area (Table 2, no reinforcing pad) becomes:

$$A_p = \frac{0.5R_i^2(L_s + a)}{0.5t_s + R_i} + 0.5d_i(L_n + t_s)$$

$$= \frac{0.5(734)^2(284.8)}{742} + 0.5(219.1)(86)$$

$$= 103395 + 9421 = 112816 \text{ mm}^2$$

The reinforcement area is:

$$A_f = t_sL_s + (L_n + t_s)t_n$$

$$= 16(154.1) + (86)(20.45)$$

$$= 2466 + 1759 = 4225 \text{ mm}^2$$

Hence :

$$\frac{A_p}{A_f} = \frac{112816}{4225} = 26.7$$

markedly lower than with the original (thin-walled) nozzle assumption, since the heavier flange hub now contributes substantially more reinforcement.

Step 3 — Maximum Allowable Working Pressure:
The MAWP governed by the nozzle intersection is

$$\mathrm{MAWP}_{\mathrm{intersection}} = \frac{f_s}{(\frac{A_p}{A_f} + 0.5)} = \frac{138}{26.7 + 0.5} = 5.07\ \mathrm{MPa}$$

The MAWP of the undisturbed spherical shell is:

$$\mathrm{MAWP}_{\mathrm{shell}} = 2f_s \ln(\frac{D_o}{D_i})$$

$$= 276\ \ln(\frac{1500}{1468}) = 276(0.0216) = 5.95\ \mathrm{MPa}$$

Since:

$$5.07 < 5.95$$

the nozzle intersection governs.
For the design pressure:

$$p_d = 2.0\ \mathrm{MPa}$$

the utilization is:

$$\frac{2.0}{5.07} = 0.39 = 39\%$$

This is a substantially larger margin than with the thin-walled nozzle assumption (51%), reflecting the additional reinforcement provided by the heavier flange hub.

Step 4 — Pressure stress at the nozzle intersection:
The auxiliary parameter (Table 1, spherical shell) is

$$z = 0.5(\frac{D_o - t_s}{t_s})(\frac{A_f}{2A_p + A_f}) = 0.5 \times 92.75 \times \frac{4225}{229857} = 0.852$$

The pressure stress at the nozzle intersection is:

$$\sigma_p = \frac{2.0}{z}[\frac{p_d}{2\ln(D_o/D_i)}] = \frac{2.0}{0.852} \times \frac{2.0}{0.0432} = 2.35 \times 46.3 = 108.8\ \mathrm{MPa}$$

Step 5 — Stresses from external forces and moments:

With no pad present, t_s is used directly (no substitution) in the Table 6 auxiliary coefficients, which apply identically to cylindrical and spherical shells:

$$c_{11} = \frac{D_o - t_s}{2t_s} = \frac{1484}{32} = 46.4$$

$$c_{21} = \frac{\sqrt{c_{11}}}{\pi\, t_s d_n} = \frac{6.81}{\pi \times 16 \times 260} = 5.21 \times 10^{-4}\ \mathrm{mm}^{-2}$$

$$c_{31} = \frac{4\sqrt{c_{11}}}{\pi\, t_s d_n^2} = \frac{27.25}{\pi \times 16 \times 67.600} = 8.02 \times 10^{-6}\ \mathrm{mm}^{-3}$$

$$c_n = \frac{t_s}{t_n} = \frac{16}{20.45} = 0.782$$

For a spherical shell, the external loads are combined into resultant force and moment terms (Table 5):

$$\sigma_F = 1.75 c_{21} \mid F \mid = 9.1\ \mathrm{MPa}$$

$$\sigma_M = 1.75 c_{31} \mid M \mid = 21\ \mathrm{MPa}$$

Step 6 — Combined stress checks:

Shell at the nozzle intersection (Table 5, spherical):

$$\sigma_p + \sigma_F + \sigma_M = 108.8 + 9.1 + 21 = 138.9\ \mathrm{MPa}$$

$$138.9 \leq 2.85\mathrm{f_s} = 393.3 \text{ MPa}$$

satisfied, 35% utilization and the governing check in this example.

Nozzle Neck:

$$\sigma_p\sqrt{c_n} + (\sigma_F + \sigma_M)c_n = 108.8(0.88) + (30.1)(0.78) = 96.2 + 23.6 = 119.8 \text{ MPa}$$

$$119.8 \leq 2.85\mathrm{f_n} = 393.3 \text{ MPa}$$

satisfied, 30% utilization and the governing check in this example.

Table 12. Summary of results for the spherical-shell worked example

Check	Location	Demand	Limit	Utilisation
Pressure capacity	Nozzle intersection (MAWP)	p_d = 2.0 MPa	MAWP = 5.07 MPa	39%
Combined stress	Shell at nozzle intersection	138.9 MPa	$2.85f_s$ = 393.3 MPa	35%
Combined stress	Nozzle neck	119.8 MPa	$2.85f_n$ = 393.3 MPa	30%

All checks are satisfied. With the revised, heavier long weld-neck flange dimensions, this example now shows comparable or larger margins than the padded cylindrical example: pressure capacity utilization is 39% (versus 37% for the padded cylindrical example), the shell-intersection check is 35% (versus 39%), and the nozzle neck is 30% (versus 72%). Unlike the padded cylindrical example, where the nozzle neck governs, here the pressure capacity check governs — a direct consequence of crediting the flange's heavier hub section as local reinforcement. Together, the two worked examples illustrate the full range of the methodology — cylindrical and spherical shells, with and without reinforcing pads, and with dissimilar reinforcement materials or nozzle geometries — and show how the governing failure mode can shift between pressure capacity, shell stress, and nozzle stress depending on the specific reinforcement details.

III. CONCLUDING REMARKS

A simplified analytical methodology has been developed for assessing the structural adequacy of flush radial pressure vessel nozzles subjected to internal pressure and externally imposed piping loads. The method combines classical pressure–area reinforcement principles with simplified stress formulations to provide a unified framework for evaluating both the pressure-carrying capacity of the nozzle–shell intersection and the combined stresses arising from pressure, external forces, and bending moments.

A key contribution of the proposed approach is the explicit relationship established between the projected pressure-loaded area and the effective reinforcement area. This relationship provides a direct physical interpretation of nozzle strength and demonstrates how reinforcement geometry influences the maximum allowable working pressure of the nozzle–shell intersection. By expressing the structural behaviour in terms of readily understood geometric parameters, the methodology enables engineers to assess the effectiveness of shell thickness, nozzle dimensions, and reinforcing pads without relying on empirical stress indices or complex numerical procedures.

The introduction of effective shell and nozzle lengths through efficiency factors provides a practical means of representing localized load transfer while maintaining computational simplicity. The resulting equations are readily implemented in standard spreadsheet software and require only basic vessel geometry and loading data, making the method particularly suitable for preliminary design studies, design verification, and routine engineering calculations.

The worked example demonstrates the practical application of the methodology and illustrates its ability to distinguish between pressure capacity, shell stresses, nozzle neck stresses, and reinforcing pad behaviour. The separate evaluation of these structural components provides valuable insight into the governing failure location and supports more effective optimization of nozzle reinforcement.

The methodology is applicable to isolated flush radial nozzles on cylindrical and spherical shells, with or without reinforcing pads, provided that shear stresses resulting from transverse forces and torsional moments remain below approximately 15% of the allowable design stress. Within this range, the assumptions underlying the simplified analytical formulation remain valid and the resulting stress predictions are expected to provide conservative engineering assessments. Configurations involving significant torsional loading, closely spaced nozzles, complex shell discontinuities, or substantial nonlinear behaviour should continue to be evaluated using detailed finite element analysis or established procedures such as those presented in WRC Bulletins 107, 297, and 368.

The principal advantage of the proposed methodology lies in its transparency. Every calculated stress component can be traced directly to a corresponding geometric or loading parameter, allowing designers to understand how changes in reinforcement, shell dimensions, or applied piping loads influence the structural response. This transparency facilitates independent verification, supports engineering judgement, and promotes efficient design optimization while remaining firmly grounded in established pressure vessel design principles.

Further work should focus on systematic validation of the proposed equations against published WRC methods, finite element analyses, and experimental data covering a broad range of vessel geometries, reinforcement configurations, and loading conditions. Such studies would quantify the conservatism of the method, establish its practical limits of applicability, and provide opportunities for refining the empirical coefficients while preserving the simplicity and physical clarity of the analytical formulation.

Overall, the proposed pressure–area methodology provides a practical balance between analytical rigor and computational efficiency. It offers engineers a conservative, transparent, and readily applicable alternative for the routine assessment of nozzle loadings, thereby complementing existing pressure vessel design procedures and reducing the need for more elaborate analyses during the early stages of mechanical design and integrity assessment.

Novel Contributions: The principal novelty of this work lies in extending the pressure–area methodology for nozzle reinforcement previously developed by the author [4] beyond maximum allowable working pressure (MAWP) determination by accounting for the combined action of internal pressure and externally imposed piping loads on the nozzle, thereby enabling evaluation of the resulting stress state under realistic service conditions. To achieve this, the paper develops a unified pressure–area analytical methodology for evaluating pressure vessel nozzles subjected simultaneously to internal pressure and external forces and moments. Unlike existing procedures based on WRC Bulletins 107, 297, and 368, which primarily employ stress indices, empirical charts, or numerical interpolation, the proposed method directly relates nozzle strength to the ratio of the projected pressure-loaded area to the effective reinforcement area. This formulation leads to a simple closed-form expression for the maximum allowable working pressure (MAWP) at the nozzle–shell intersection while using the same geometric framework to evaluate pressure stresses, external forces, and bending moments. The methodology further introduces effective shell and nozzle participation lengths through efficiency factors, incorporates the contribution of reinforcing pads together with verification of the pad-to-shell transition, and provides a transparent set of equations that can readily be implemented in standard engineering spreadsheets. The resulting procedure offers a computationally efficient and conservative alternative for routine engineering assessment while preserving the fundamental mechanics governing nozzle–shell interaction.

REFERENCES

[1] Wichman, K. R., Hopper, A. G., and Mershon, J. L., 1965. *Local Stresses in Spherical and Cylindrical Shells Due to External Loadings*. WRC Bulletin No. 107. New York, NY: Welding Research Council.

[2] Rodabaugh, E. C., Ranjan, G. V., Mershon, J. L., and Mokhtarian, K., 1987. *Local Stresses in Cylindrical Shells Due to External Loadings on Nozzles—Supplement to WRC Bulletin No. 107 (Revision I)*. WRC Bulletin No. 297. New York, NY: Welding Research Council.

[3] Mokhtarian, K., and Endicott, J. S., 1991. *Stresses in Intersecting Cylinders Subjected to Pressure*. WRC Bulletin No. 368. New York, NY: Welding Research Council.

[4] Stikvoort, W. J., 2025. "The Pressure Area Method (PAM) for Nozzle Reinforcement in Pressure Vessels: Theory, Application, and Design Implications." *International Journal of Multidisciplinary Science and Management*, Vol. 2, No. 4, pp. 1–7.

[5] C.J.Dekker,H.J.Bos: Nozzles on external loads and internal pressure Int. Journal of PressureVessels & Piping, 1997, 72, 1-18.

AUTOBIOGRAPHY

Walther Stikvoort is an independent Subject Matter Expert in Pressure Equipment Design and Integrity with over 50 years of experience in the mechanical design, assessment, and fitness-for-service evaluation of pressure vessels, piping systems, and related process equipment. His areas of expertise include pressure vessel design, nozzle reinforcement, piping load assessment, local stress analysis, and structural integrity in accordance with internationally recognised design codes and standards. His current work focuses on the development of practical analytical methods that simplify complex engineering assessments while maintaining sound theoretical foundations and conservative design principles. As an independent consultant, he has supported equipment manufacturers, engineering contractors, and owner-operators in resolving challenging mechanical design and integrity issues. His technical publications emphasize transparent, efficient engineering methodologies for routine design verification and pressure equipment integrity assessment.

AUTOBIOGRAPHY

Farzad Gardaneh is a Senior Static Equipment Engineer with more than 12 years of experience specializing in the design, analysis, and integrity assessment of static process equipment for the oil, gas, petrochemical, and energy industries. His expertise encompasses the design and evaluation of pressure vessels, storage tanks, piping interfaces, and finite element analysis (FEA).

His research and professional interests focus on nozzle penetrations and reinforcement design in pressure vessels, including the attenuation of stress disturbances around nozzles, conventional and alternative methodologies for nozzle load evaluation, probabilistic frameworks for early-stage pressure vessel and piping design, and stress intensity assessment under both operating and hydrostatic test conditions. His work integrates rigorous analytical methods with the practical application of international design codes, reflecting a career dedicated to advancing pressure vessel mechanics, fatigue assessment, structural integrity, and equipment reliability.